Procedural learning is associated with microstructure of basal ganglia-cerebellar circuitry in children

Brain and Cognition 180 (2024) 106204

Contents lists available at ScienceDirect

Brain and Cognition

journal homepage: www.elsevier.com/locate/b&c

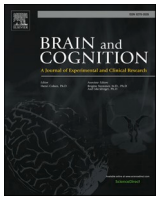

Procedural learning is associated with microstructure of basal ganglia-cerebellar circuitry in children

Kaila M. Bianco [a,*], Ian Fuelscher [a], Jarrad A.G. Lum [a], Mervyn Singh [a], Pamela Barhoun [a], Timothy J. Silk [a,b], Karen Caeyenberghs [a], Jacqueline Williams [c], Peter G. Enticott [a], Mugdha Mukherjee [a], Gayatri Kumar [a], Jessica Waugh [a], Christian Hyde [a]

[a] Cognitive Neuroscience Unit, School of Psychology, Deakin University, Geelong, Australia
[b] Developmental Imaging, Murdoch Children's Research Institute, Melbourne, Australia
[c] Institute for Health and Sport, College of Sport and Exercise Science, Victoria University, Melbourne, Australia

A B S T R A C T

In adults, individual differences in procedural learning (PL) are associated with white matter organization within the basal ganglia-cerebellar circuit. However, no research has examined whether this circuitry is related to individual differences in PL during childhood. Here, 28 children (M_{age} = 10.00 ± 2.31, 10 female) completed the serial reaction time (SRT) task to measure PL, and underwent structural magnetic resonance imaging (MRI). Fixel-Based Analysis was performed to extract specific measures of white matter fiber density (FD) and fiber cross-section (FC) from the superior cerebellar peduncles (SCP) and the striatal premotor tracts (STPMT), which underlie the fronto-basal ganglia-cerebellar system. These fixel metrics were correlated with the 'rebound effect' from the SRT task – a measure of PL proficiency which compares reaction times associated with generating a sequence, to random trials. While no significant associations were observed at the fixel level, a significant positive association was observed between average FD in the right SCP and the rebound effect, with a similar trend observed in the left SCP. No significant effects were detected in the STPMT. Our results indicate that, like in adults, microstructure of the basal ganglia-cerebellar circuit may explain individual differences in childhood PL.

1. Introduction

Our ability to implicitly acquire and apply motor sequences is essential to daily living, and particularly important for skill acquisition during childhood. This process, known as procedural learning (PL), is necessary for performing fundamental motor tasks such as tying shoelaces, riding a bike, and typing on a keyboard. The PL process is not only central to the expression of motor skills (Ashe et al., 2006; Doyon et al., 2009), but may also support higher-order operations, including language and social skills (Lieberman, 2000; Ullman & Pierpont, 2005). Furthermore, atypical PL is often reported in children with neurodevelopmental disorders where motor skills are delayed (Clark & Lum, 2017; Van Dyck et al., 2022). Given the critical role that PL plays in the maturation of core motor, cognitive and social processes, it is essential to understand the neural mechanisms that underpin this process in children.

PL has been widely studied using the serial reaction time (SRT) task (Nissen & Bullemer, 1987). Here, a visual stimulus appears repeatedly in one of four spatial locations on a computer screen, and participants press buttons on a response panel that matches the stimulus' location. Participants are not informed that the stimuli are presented in a predetermined, repeating visuospatial sequence. In typically developing participants, manual reaction times (RTs) decrease (i.e., become faster) across these trials, which is generally interpreted as the consequence of learning the repeating sequence. Following presentation of the 'sequence blocks', a block of random trials is then presented. Implicit learning across the initial sequence blocks is inferred if the observed initial reduction in RTs is followed by an increase in RT at the introduction of the 'random block'. The magnitude of the increase in RT between the final sequence block and the random block is referred to as the 'rebound effect' and is used to measure PL proficiency (Janacsek & Nemeth, 2013; Robertson, 2007). Participants who are more sensitive to the sequence embedded in the task typically exhibit a larger rebound effect, which indicates that RTs were faster on the sequence block compared to random.

To date, the neural basis of PL has predominantly been explored in adults, which has implicated fronto-basal ganglia-cerebellar circuitry. For example, Activation Likelihood Estimation meta-analyses of functional MRI studies revealed robust activation in the basal ganglia, cerebellum, and premotor regions during SRT task performance in

* Corresponding author at: Deakin University, Level 5, Building BC, 221 Burwood Hwy, Burwood VIC 3125, Australia.
E-mail address: kbianco@deakin.edu.au (K.M. Bianco).

https://doi.org/10.1016/j.bandc.2024.106204
Received 10 April 2024; Received in revised form 7 July 2024; Accepted 8 July 2024
Available online 24 July 2024

neurotypical adults (Baetens et al., 2020; Janacsek et al., 2020). The proposed involvement of these (sub)cortical regions in sequence learning is broadly consistent with previous theoretical and behavioral models of PL (Doyon et al., 2003; Penhune & Steele, 2012), as well as neuropsychological accounts which show deficits in PL in patients with neurological disease affecting the basal ganglian circuitry (Parkinson's Disease e.g., Siegert et al., 2006; Huntington's Disease e.g., Knopman & Nissen, 1991; cerebellar damage e.g., Morgan et al., 2021). While the available neuroimaging evidence has examined the neural correlates of PL in terms of functional activation, our group recently demonstrated that microstructural organization within white matter tracts connecting fronto-basal ganglia-cerebellar regions explains individual differences in PL in adults (Bianco et al., 2023). In this recent work, we used the SRT task to measure PL, and adopted a novel Fixel-Based Analysis (FBA) framework to generate fiber specific estimates of micro- and macro-structure within those tracts that support communication between fronto-basal ganglia-cerebellar regions previously implicated in PL. These included the superior cerebellar peduncles (SCP), and the striatal-premotor tracts (STPMT). We found that increased fiber density within the SCP was associated with a larger rebound effect. These study findings support broader evidence of involvement of basal ganglia-cerebellar systems in PL in adults, extending earlier accounts by suggesting a relationship between white matter network structure and PL ability. The current study investigated whether this also extends to children.

To our knowledge, no study to date has considered the role of white matter organization in PL in typically developing children. Childhood is a particularly sensitive period for neuro-cognitive development, whereby genetic (and neurobiological) factors constantly interact with experience to alter structural connectivity (Edde et al., 2021). As such, the white matter properties of a dynamic child brain are not necessarily comparable to that of a mature adult brain, particularly in the case of white matter which is known to transform across the lifespan (for review, see Lebel et al., 2019). Despite some similarities in the functional regions implicated in PL between children and adults (Baetens et al., 2020; Janacsek et al., 2020; Thomas et al., 2004), we cannot assume that the structural (i.e., white matter) properties that support adult PL are necessarily analogous to children. There remains a need to investigate the role of fronto-basal ganglia-cerebellar circuitry in childhood PL. Doing so may provide insight into the mechanisms that explain differences in children's abilities to engage in PL, and why PL presents atypically in some children.

The aim of the current study was to investigate the role of white matter organization in fronto-basal ganglia-cerebellar tracts in PL in typically developing children. We administered the SRT task to measure PL in children aged 6–14 years. A subset of children underwent higher-order diffusion magnetic resonance imaging (MRI), following which FBA was conducted to characterize white matter organization in vivo. Like our work in adults (Bianco et al., 2023), we delineated white matter tracts that support communication within the fronto-basal ganglia-cerebellar system. Tracts of interest included the STPMT, which connects the premotor and basal ganglia network; and the SCP, which connects the cerebellum and basal ganglia network. Specific measures of fiber density (FD; a measure of the microscopic density of a given fiber population), and fiber cross section (FC; a measure of the macroscopic cross-section region occupied by a given fiber bundle) were extracted within each tract, and we probed the association between these metrics and the rebound effect on the SRT task. We hypothesized that FD and FC in the SCP and STPMT would be positively associated with the rebound effect (i.e., PL) in typically developing children.

2. Methods

2.1. Participants

Participants were 37 children aged 6–14 years ($M_{age} = 9.97 \pm 2.32$, 13 female, 19% left-handed), recruited via flyers posted on community boards and on social media. Of these participants, a subset of 28 children also underwent MRI ($M_{age} = 10.00 \pm 2.31$, 10 female, 18% left-handed). Exclusionary criteria were a known medical or neurodevelopmental condition that might be expected to impact PL (e.g., autism spectrum disorder or dyslexia) and, for those who participated in MRI, contra-indications to MRI (e.g., claustrophobia or metal in the body). All parents provided written informed consent, while children gave assent and were reimbursed for their participation. The Deakin University Human Research Ethics Committee approved the experimental procedures (2019–009).

We note that preliminary analyses revealed no significant differences in RT across blocks ($F = 0.67$, $p = .420$) – or the rebound effect ($t = 0.32$, $p = .754$) – between left- and right-handed participants. As such, our data indicated that handedness did not impact SRT task performance, so data were collapsed across left- and right-handed participants.

2.2. Serial reaction time (SRT) task

The SRT task was presented using E-Prime 2 software (Psychology Software Tools, Pittsburgh, PA). Participants were seated in front of a 17-inch display and operated a game controller consisting of four buttons arranged in the shape of a diamond (see Fig. 1). At the beginning of a trial, participants viewed a white screen with four empty diamond-arranged boxes for 500 ms. Then, a visual stimulus (shape) appeared in one of the four boxes, and participants responded as quickly as possible by pressing the button on the controller that corresponded to the stimulus' location. Following each response, feedback was given in the form of a red border appearing over the indicated box. Failure to respond to the stimuli within 800 ms was coded as an incorrect response. These events represented one trial. The task consisted of four blocks of 60 trials. Each block was separated by a 3-second rest period in which a white screen appeared on the display.

Participants were unaware that on Blocks 1–3, the visual stimulus' location followed a pre-determined 10-element sequence. Labelling the left-most point of the diamond configuration as 1, and moving anti-clockwise around the diamond configuration, the sequence was 3-4-1-2-4-1-3-4-2-1. The sequence repeated six times to equal 60 trials in each sequence block. On Block 4, the visual stimulus appeared pseudo-randomly in one of the four positions on the display (totaling 60 trials) adhering to the following constraints: 1) the visual stimulus could not appear in the same location on two consecutive trials; 2) the number of times the visual stimulus appeared in each of the four spatial locations was the same as for the sequence blocks; 3) the frequency of each pairwise transition in the random block matched the sequence blocks. The randomization was reset at the end of each ten trials.

The stimuli comprised 60 different shapes (circles and polygons),

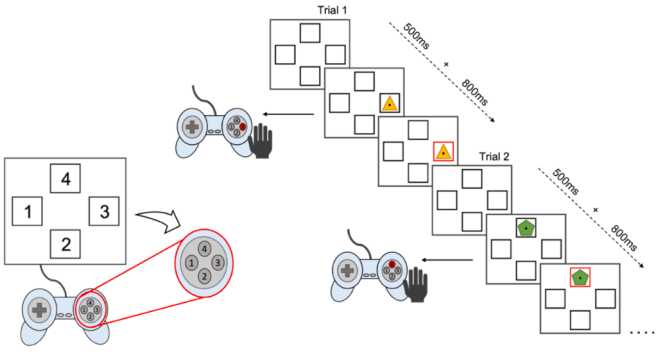

Fig. 1. Schematic overview of the serial reaction time (SRT) task (adapted from Lum et al., 2010). Left: shows the locations that the visual stimuli could appear on each trial, and the corresponding buttons on the controller used as the response device. Right: provides timing details on two trials.

presented in different colors (purple, green, blue, red, orange). On each trial within a block, a different visual stimulus appeared on the screen, without replacement. This aided in disguising the sequence, thus reducing the likelihood that participants would become aware of it (Koch et al., 2020; Lum, 2020). This was important, since explicit learning appears to rely on different neural substrates compared to implicit learning (see Hardwick et al., 2013).

2.3. Diffusion MRI acquisition

A subset of children ($N = 28$, $M_{age} = 10.00 \pm 2.31$, 10 female, 19% left-handed) underwent MRI scanning at the Florey Institute of Neuroscience and Mental Health, Heidelberg, using a Siemens Prisma 3T MRI scanner (Erlangen, Germany). Children were screened for MRI contraindicators, and those who were eligible underwent a mock scan to help them acclimate to the MRI environment and reduce any anxiety about the scanning session. High resolution T1-weighted multi-echo MPRAGE images were acquired for each participant using the following parameters: TR = 1900 ms, TI = 900 ms, TE = 2.49 ms, flip angle = 9°, voxel size = 0.9 mm^3, acquisition matrix 256 × 256, FoV = 240 mm, 192 contiguous slices.

Multi-shell high angular resolution diffusion imaging (HARDI) was acquired following a single-refocused echo planar imaging (EPI) sequence with the following parameters: 84 axial slices; 1.8 mm isotropic voxels; TE/TR = 98 ms/3275 ms; flip angle = 90°; acquisition matrix 128 × 128, multiband (MB) acceleration factor = 4; phase encoding anterior-posterior (AP); and SENSE1 multi-coil reconstruction. The diffusion weighting schedule included b-values = 0, 1600, 5000, with 8, 25, 64 volumes respectively. Half of the volumes were acquired in the A≫P, and half in the P≫A phase encoding directions. Additionally, we also acquired the corresponding phase images for complex bias data denoising (Cordero-Grande et al., 2019).

2.4. MRI processing

2.4.1. Pre-processing

Diffusion data were processed using the MRtrix3 software package (Tournier et al., 2019). Prior to pre-processing, the quality of the raw images was visually assessed. Here, one participant was excluded for substantial signal dropout. Pre-processing included denoising (Veraart et al., 2016), removal of Gibbs ringing (Kellner et al., 2016), and eddy and motion distortion correction (Andersson et al., 2016). Magnitude and phase data was exported to facilitate complex data denoising (Cordero-Grande et al., 2019). Data were then upsampled to an isotropic voxel size of 1.50 mm^3 before the computation of brain masks. Brain masks were inspected for holes, resulting in the removal of one participant ($N = 26$).

2.4.2. Fiber orientation distribution calculation

Response functions were estimated for gray matter, white matter, and cerebrospinal fluid, and then averaged across participants to generate group-level response functions for each tissue type (Dhollander et al., 2019). Using these group average response functions, multi-shell multi-tissue constrained spherical deconvolution (MSMT-CSD) was performed for each participant to generate individual fiber orientation distribution (FOD) maps (Jeurissen et al., 2014). FOD maps then underwent multi-tissue informed bias field and intensity normalization, so that the FOD magnitudes were comparable between participants (Raffelt et al., 2017). A study-specific population template using FOD maps from all 26 participants was then generated. Each participant's individual FOD map was subsequently registered to the population template and segmented to produce individual fixel maps for each participant (Raffelt et al., 2017).

2.4.3. Fixel metric calculations

Fixel metrics (FD and FC) were computed for each participant across all white matter fixels, as described in Raffelt et al. (2017). Of note, FC (herein referred to as logFC) was log-transformed as per the MRtrix3 suggestion for FC-based statistical analyses to ensure data is normally distributed (see www.mrtrix.org). FD and logFC metrics were used for further analyses.

2.4.4. Tracts of interest

As in our previous study (Bianco et al., 2023), the semi-automated TractSeg tool was used to delineate the SCP and STPMT (Wasserthal et al., 2018, 2019). TractSeg offers a balance between the accuracy of manual delineation, and the reliability of atlas-based approaches (Genc et al., 2020). TractSeg was applied to the study-specific population template to segment those voxels corresponding to the SCP (left and right) and STPMT (left and right) in each individual. In this way, the derived tracts aligned closely with the structural neuroanatomy of the participants in the sample. These tractograms were subsequently combined across hemispheres to generate a single bilateral tractogram for each tract (Fig. 2). The SCP and STPMT tractograms were then converted to fixel maps, whereby each participant's FD and FC fixel maps were cropped to only include fixels belonging to the SCP and STPMT using the *'tck2fixel'* command (Tournier et al., 2019). The tract-specific fixel masks were then smoothed to generate fixel-fixel connectivity matrices using the *'fixelfilter'* command (Tournier et al., 2019). The smoothed fixel matrices for the SCP and STPMT were then submitted for statistical analysis.

2.5. Statistical analyses

Analyses of SRT task data were conducted primarily using the 'tidyverse' (Wickham et al., 2019) and 'lme4' (Bates et al., 2014) packages in R (R Core Team, 2022). Graphs were created using the 'ggplot2' (Wickham, 2011) and 'sjPlot' (Lüdecke & Lüdecke, 2015) packages. Herein, sequence blocks 1, 2 and 3 will be referred to as S1, S2 and S3, and the fourth random block will be referred to as R1.

2.5.1. Behavioral analysis

Both accuracy and RT were measured for the SRT task. A correct response was recorded when a participant pressed the button on the controller that matched the location of the visual stimulus. For each participant, the proportion of correct responses was computed for each block (i.e., S1, S2, S3, R1). RT, in milliseconds, measured the time taken to press the correct button on the controller following stimulus onset. Only RTs from correct responses were included in the analyses. For each participant, mean RTs for each block were calculated.

To confirm that the predicted PL effects took place during SRT task performance, preliminary analyses were conducted on the full sample ($N = 37$). We conducted a linear mixed model (LMM) using restricted estimation maximum likelihood (REML), with mean RT as the dependent variable, and with age and block (S1 vs. S3; see also Bianco et al., 2023; Lum et al., 2019) as fixed effects. REML is known to provide less biased estimates, particularly when estimating modest sample sizes, compared to alternative models such as maximum likelihood (ML) which often require larger sample sizes to generate unbiased models (Maestrini et al., 2024). Trend analysis was also conducted to assess whether participants showed a linear trend in RT performance from S1 to S3, with a significant reduction expected where sequence learning had taken place.

To investigate the rebound effect on the SRT task, we ran a LMM using REML, with RT as the dependent variable, and with age and block (S3 vs. R1) as fixed effects. Trend analysis was also conducted to assess whether participants showed a linear increase in RT from S3 to R1, indicating a rebound effect. The above models each contained a random intercept to account for clustering of RT in each block within individuals (i.e., the model inherently controlled for individual differences in RT).

Since these preliminary analyses suggested that PL had taken place, we next calculated a single rebound effect metric for each participant,

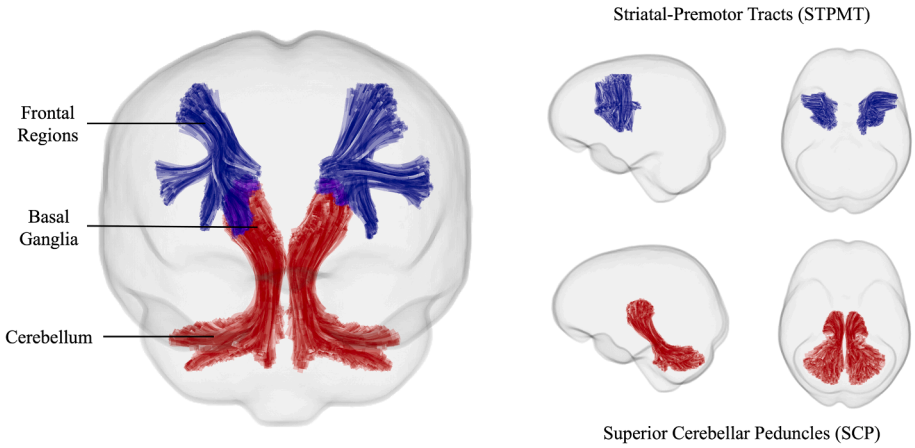

Fig. 2. Glass brain depicting the SCP and STPMT, delineated using TractSeg (Wasserthal et al., 2018, 2019). The tractograms from the left and right hemispheres were combined to generate one single bilateral tractogram for each tract (SCP in red, STPMT in blue). Labels indicate the cortical and subcortical regions that the white matter tracts connect. Glass brain created in MRtrix3 (Tournier et al., 2019). (For interpretation of the references to colour in this figure legend, the reader is referred to the web version of this article.)

which was subjected to subsequent analyses as the dependent measure of PL (Bianco et al., 2023; Knopman & Nissen, 1991; Lum et al., 2019; Robertson, 2007; Siegert et al., 2006). Here, raw RTs for each trial were first transformed to z-scores to control for general processing speed (Janacsek et al., 2012; Koch et al., 2020). This was calculated for each participant based on their mean and standard deviation RT for all trials across all blocks. This transformation ensured that, across participants, the shortest and longest RTs had similar values. This allowed us to attribute participant differences in the magnitude of the rebound effect to PL only, rather than individual difference effects in general processing speed (i.e., RT alone). Then, mean z-scores were calculated for each block, resulting in a mean z-score for RT for each block, for each participant. The magnitude of the rebound effect was calculated for each participant by subtracting the mean z-score for RT for S3 from the mean z-score for RT for R1.

2.5.2. Fixel-based analysis

To investigate the relationship between individual differences in SRT task performance and white matter organization within the SCP and STPMT, the connectivity-based fixel enhancement (CFE) method in MRtrix3 was initially used to probe the relationship between the rebound effect on the SRT task and fixel-based metrics in the SCP and STPMT ($N = 26$). CFE provides a permutation-based, family-wise error corrected p-value for every individual fixel in the population template space (Raffelt et al., 2015). Sex and age were included as covariates, and we further controlled for intracranial volume (ICV) for analyses involving FC (Smith et al., 2019). ICV was derived from each subject's structural T1 image using FreeSurfer (Fischl, 2012).

As noted in the Results section below, our CFE analyses failed to detect significant associations between fixel based metrics and the rebound effect, though we observed trend effects at the fixel level for FD in the right SCP (see Supplementary 1). As per our comparable work examining white matter correlates of PL in adults (Bianco et al., 2023), we explored this trend using a tract-based ROI analysis. This analysis examined the association between white matter fiber metrics (averaged across all fixels) and the standardized rebound effect. These associations were calculated separately for the left SCP and right SCP. Covariates included sex and age. These results are reported in the manuscript proper.

3. Results

3.1. SRT task performance

Relevant assumptions of multicollinearity (variance inflation factors [VIFs] < 5), linearity (scatterplots), homoscedasticity (homogeneity of residuals plot) and normality (residual histograms and Q-Q plots) were met for RT data.

The mean proportion of correct responses for all blocks approached ceiling (S1: $M = 0.92$, $SE = 0.01$; S2: $M = 0.93$, $SE = 0.02$; S3: $M = 0.92$, $SE = 0.01$; R1: $M = 0.90$, $SE = 0.02$). Mean RTs for each block are presented in Fig. 3. The LMM exploring RT from S1 to S3 revealed a significant contribution of age to the variation in RT, $B = -22.64$, $SE = 3.14$, $t(35) = -7.21$, $p < .001$. After controlling for age, trend analysis showed a significant linear main effect for block, $B = -19.73$, $SE = 4.89$, $t(36) = -4.03$, $p < .001$, whereby RT decreased significantly from S1 ($M = 456.91$, $SD = 75.47$) to S3 ($M = 429.02$, $SD = 66.25$).

The LMM exploring the rebound effect (i.e., change in RT from S3 to R1) revealed a significant contribution of age to the variation in RT, $B = -22.53$, $SE = 2.90$, $t(35) = -7.77$, $p < .001$. After controlling for age, trend analysis showed a significant linear main effect for block, $B = 36.54$, $SE = 4.05$, $t(36) = 9.03$, $p < .001$, whereby RT increased significantly from S3 ($M = 429.02$, $SD = 66.25$) to R1 ($M = 480.69$, $SD =$

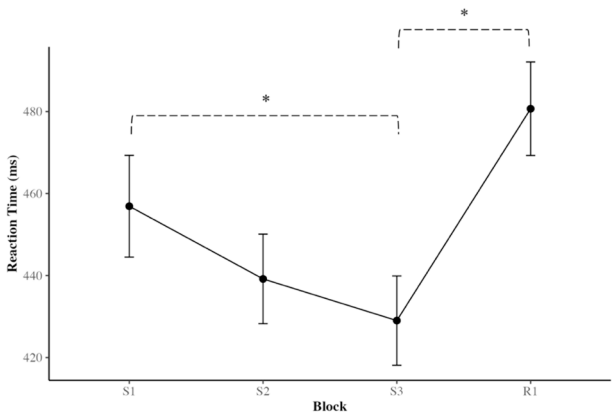

Fig. 3. Mean reaction times (RTs) on the SRT task reported by Block ($N = 37$). Error bars show standard error. S1, S2 and S3 represent blocks 1, 2 and 3, where the stimuli were presented in a visuospatial sequence. R1 represents the fourth block, where stimuli were presented in a random visuospatial order. * = statistically significant difference at $p < 0.001$.

69.36).

3.2. Association between the rebound effect and fixel-based metrics

As can be seen in Fig. 4, there was a significant positive correlation between mean FD in the right SCP and the standardized rebound effect ($r = 0.41$, $p = .049$). The association between mean FD in the left SCP and the standardized rebound effect fell short of statistical significance ($r = 0.35$, $p = .098$).

4. Discussion

The current study examined the structural basis of PL within fronto-basal ganglia-cerebellar circuitry in children. The main finding was that greater average FD in the right SCP was associated with better PL on the SRT task, as indexed by the magnitude of the rebound effect. There was also a trend towards an association between mean FD in the left SCP and the rebound effect. We did not observe an association between logFC in the SCP and the rebound effect, nor any relationships between micro/macrostructure in the STPMT and the rebound effect. These findings broadly align with findings from adults (Bianco et al., 2023), suggesting basal ganglia-cerebellar microstructure may underlie individual differences in PL across the lifespan.

As expected, behavioral patterns on the SRT task indicated that PL took place in our sample of children (Nissen & Bullemer, 1987; Robertson, 2007). That being, participant RTs became progressively faster across sequence blocks, and slowed significantly when a random sequence was presented. This pattern is characteristic of PL on the SRT task in typically developing children (Gheysen et al., 2011; Lum et al., 2010) as well as in neurotypical adult populations (Bianco et al., 2023). Given this, we were confident that the magnitude of the rebound effect (i.e., the difference in RT between the final sequence block and random block) provided a reliable measure of PL for the current study.

At the fixel level, we did not observe significant associations between the rebound effect and white matter organization in the SCP or STPMT. Still, when averaging FD across the entire SCP, we found a significant positive association, whereby FD in the right SCP was associated with a larger rebound effect on the SRT task. The same trend was also present in the left SCP ($p = .098$). FD is thought to reflect axon count and/or density within a voxel, which seems to be related to the speed of information transfer within a tract (Raffelt et al., 2017). Our exploratory results therefore suggest that SRT task performance may be more proficient in those children where the basal ganglia-cerebellar white matter pathway endows a bundle with greater information processing capacity, making it more efficient (Fletcher et al., 2021; Horowitz et al., 2015). These findings mirror those of our recent adult study, which also found a positive association between FD in segments of both the left and right SCP and PL in a sample of adults (Bianco et al., 2023). Further, we found no relationship between logFC in the SCP and the rebound effect, which may suggest that PL is predominantly driven by microstructural properties within the basal ganglia-cerebellar circuit, rather than overall tract macrostructure – another finding that mirrors our adult work (Bianco et al., 2023). Whilst speculative in the absence of a direct quantitative comparison between child and adult data, we tentatively propose that the overlap between child and adult results may suggest that the relationship between the basal ganglia-cerebellar circuit and PL is established early in development, and may be age-invariant from mid-childhood.

In the STPMT, there were no significant correlations detected between white matter organization (FD and logFC) and PL (rebound effect). This finding, or lack thereof, aligns with what we observed in our sample of adults (Bianco et al., 2023), which may suggest that white matter organization in these regions is not linked to individual differences in PL. However, given our modest sample size, it may be that we were not optimized (or sufficiently powered) to detect small effects. Further, while we controlled for the effects of age, we acknowledge that the age span adopted in the present study (6–14 years) is a period of rapid white matter maturation (Lebel et al., 2019). Thus, it is possible that the effects of interest may alter as a function of age across this span – an effect that we were underpowered to probe, but should be the focus of future work. In all, a lack of effects found in the present study should not be taken as evidence of a true null effect, and the association between PL and white matter organization in the STPMT warrants further consideration with a larger sample. At a minimum, our evidence here suggests that the observed effects of white matter on PL may be stronger in the SCP than in the STPMT, which appears to be a consistent pattern in both children and adults.

The findings presented here contribute to our understanding of the microstructural correlates of childhood PL and may have practical implications for future research. We report qualified evidence that in typically developing children, greater FD in the SCP was associated with better SRT task performance. As such, white matter organization within the basal ganglia-cerebellar network may offer a window into the mechanisms that subserve compromised PL when it emerges in childhood. Further, PL difficulties have been implicated in the symptom profile of several neurodevelopmental disorders e.g., developmental coordination disorder (Van Dyck et al., 2022) and specific language impairment (Lum et al., 2014). While speculative, our findings may signal involvement of basal ganglia-cerebellar circuitry in those developmental instances where PL is compromised. This suggestion is supported by neuroimaging evidence reporting atypical cerebellar structures in these disorders (Gill et al., 2022; Hodge et al., 2010; Shaw et al., 2016). Future research should explore this suggestion further.

The current study is not without limitations. First, we failed to detect our effects of interest within the fronto-basal-cerebellar network at the fixel level. We argue that this may have occurred due to a lack of power, given the trend effects observed at the fixel level (see Supplementary 1), and that we proceeded to detect effects at the whole tract level. Still, it is

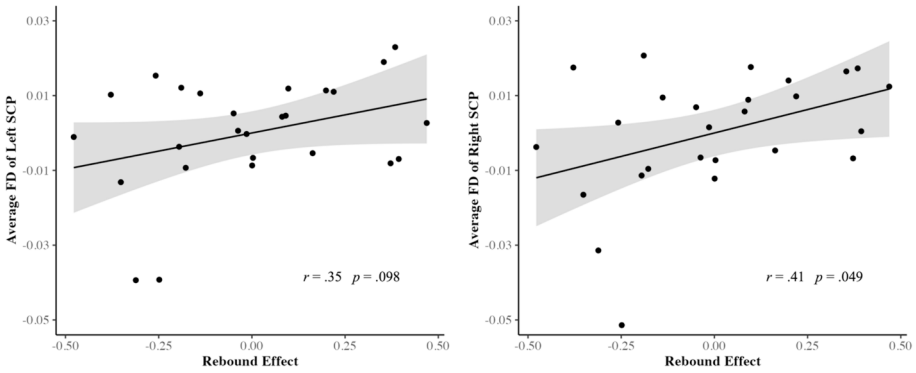

Fig. 4. Scatterplots visualizing the association between mean FD and the standardized rebound effect for the left and right SCP ($N = 26$). Residualized values are presented after controlling for sex and age. The shaded area represents standard error.

interesting to note that the pattern of effects observed here in children overlaps with those we observed in adults, particularly our findings implicating the SCP in PL. In this context, and with consideration of the scatterplots, the pattern of effects observed at the whole tract level appears to be robust. Further, while the tract average approach taken here is common, it does not allow for inferences to be drawn about if (or how) this effect changes within, or along, our tracts of interest (i.e., the SCP). With all this in mind, we recommend that larger cohorts be examined in future studies to better ascertain how the relationship between white matter organization and PL in children manifests at the fixel level.

Additionally, we chose to investigate the role of the SCP and STPMT in PL since they underlie the fronto-basal ganglia-cerebellar circuit that prior functional work has implicated in PL (Baetens et al., 2020; Janacsek et al., 2020). We do, however, acknowledge that additional white matter tracts, such as the middle cerebellar peduncle (MCP; Palesi et al., 2017), likely contribute to PL. To minimize the number of comparisons and maintain study sensitivity, we did not include this tract in our analyses (nor other potential candidate white matter tracts). Future work should consider the broader role of white matter networks – including the MCP – in SRT task performance in children, to develop a unified neurocognitive account of PL in children.

Lastly, we acknowledge that the age range of our sample (6–14 years) spans a large developmental period, during which white matter organization undergoes significant maturation (Lebel et al., 2019). As such, it is possible that the association between white matter microstructure and the rebound effect may differ as a function of age. While not a direct aim of the study, we were nonetheless underpowered to address this question specifically. However, we controlled for age in our analyses, and we observed no significant association between age and the rebound effect ($r = -0.23$, $p = 0.264$). Hence, we can be confident that the observed relationship between cerebellar morphology and SRT task performance in the present study cannot, at least solely, be attributed to maturational factors related to age in the 6-to-14-year span. Furthermore, as per the recommended pipeline (Smith et al., 2019), analyses involving FC corrected for brain volume (i.e., ICV), to account for differences in volumetric changes across our participants. Thus, given that age and ICV were corrected for, we can be confident that our results do not, at least solely, reflect any age-related differences in morphology.

To conclude, this is the first study to explore the association between white matter micro/macrostructure and PL in typically developing children. We observed a significant positive association between PL and white matter microstructure in the right SCP in children, with a similar trend observed for the left SCP. Specifically, greater average FD within these tracts was associated with better PL on the SRT task. This effect overlaps with what we observed in neurotypical adults. Our findings provide qualified support for the role of white matter organization in the basal ganglia-cerebellar circuit in explaining individual differences in childhood PL.

CRediT authorship contribution statement

Kaila M. Bianco: Writing – review & editing, Writing – original draft, Visualization, Project administration, Methodology, Investigation, Formal analysis, Conceptualization. **Ian Fuelscher:** Writing – review & editing, Supervision, Project administration, Methodology, Funding acquisition, Formal analysis, Conceptualization. **Jarrad A.G. Lum:** Writing – review & editing, Supervision, Project administration, Funding acquisition, Formal analysis. **Mervyn Singh:** Writing – review & editing, Project administration, Formal analysis. **Pamela Barhoun:** Writing – review & editing, Project administration, Formal analysis. **Timothy J. Silk:** Writing – review & editing, Funding acquisition. **Karen Caeyenberghs:** Writing – review & editing, Funding acquisition. **Jacqueline Williams:** Writing – review & editing, Funding acquisition. **Peter G. Enticott:** Writing – review & editing, Funding acquisition. **Mugdha Mukherjee:** Writing – review & editing, Project administration. **Gayatri Kumar:** Writing – review & editing, Project administration. **Jessica Waugh:** Writing – review & editing, Project administration. **Christian Hyde:** Writing – review & editing, Visualization, Supervision, Project administration, Methodology, Investigation, Funding acquisition, Formal analysis, Conceptualization.

Declaration of competing interest

The authors declare that they have no known competing financial interests or personal relationships that could have appeared to influence the work reported in this paper.

Data availability

The authors do not have permission to share data.

Acknowledgements

This work was supported by a Child Development Fund Research Grant from the Waterloo Foundation (Ref no. 2013-3613).

Appendix A. Supplementary data

Supplementary data to this article can be found online at https://doi.org/10.1016/j.bandc.2024.106204.

References

Andersson, J. L., Graham, M. S., Zsoldos, E., & Sotiropoulos, S. N. (2016). Incorporating outlier detection and replacement into a non-parametric framework for movement and distortion correction of diffusion MR images. *Neuroimage, 141*, 556–572. https://doi.org/10.1016/j.neuroimage.2016.06.058

Ashe, J., Lungu, O. V., Basford, A. T., & Lu, X. (2006). Cortical control of motor sequences. *Current Opinion in Neurobiology, 16*(2), 213–221. https://doi.org/10.1016/J.CONB.2006.03.008

Baetens, K., Firouzi, M., Van Overwalle, F., & Deroost, N. (2020). Involvement of the cerebellum in the serial reaction time task (SRT) (Response to Janacsek et al.). In *NeuroImage* (Vol. 220). Academic Press Inc. Doi: 10.1016/j.neuroimage.2020.117114.

Bates, D., Mächler, M., Bolker, B. M., & Walker, S. C. (2014). Fitting Linear Mixed-Effects Models using lme4. *Journal of Statistical Software, 67*(1). https://doi.org/10.48550/arxiv.1406.5823

Bianco, K. M., Fuelscher, I., Lum, J. A. G., Singh, M., Enticott, P. G., Caeyenberghs, K., & Hyde, C. (2023). Individual differences in procedural learning are associated with fiber specific white matter microstructure of the superior cerebellar peduncles in healthy adults. *Cortex, 161*. https://doi.org/10.1016/j.cortex.2023.01.006

Clark, G. M., & Lum, J. A. G. (2017). Procedural learning in Parkinson's disease, specific language impairment, dyslexia, schizophrenia, developmental coordination disorder, and autism spectrum disorders: A second-order meta-analysis. *Brain and Cognition, 117*, 41–48. https://doi.org/10.1016/J.BANDC.2017.07.004

Cordero-Grande, L., Christiaens, D., Hutter, J., Price, A. N., & Hajnal, J. V. (2019). Complex diffusion-weighted image estimation via matrix recovery under general noise models. *NeuroImage, 200*. https://doi.org/10.1016/j.neuroimage.2019.06.039

Dhollander, T., Mito, R., Raffelt, D., & Connelly, A. (2019). Improved white matter response function estimation for 3-tissue constrained spherical deconvolution. *Proceedings of the International Society for Magnetic Resonance in Medicine, May 11-16*.

Doyon, J., Bellec, P., Amsel, R., Penhune, V., Monchi, O., Carrier, J., Lehéricy, S., & Benali, H. (2009). Contributions of the basal ganglia and functionally related brain structures to motor learning. *Behavioural Brain Research, 199*(1), 61–75. https://doi.org/10.1016/J.BBR.2008.11.012

Doyon, J., Penhune, V., & Ungerleider, L. G. (2003). Distinct contribution of the cortico-striatal and cortico-cerebellar systems to motor skill learning. In. *Neuropsychologia, 41*.

Edde, M., Leroux, G., Altena, E., & Chanraud, S. (2021). Functional brain connectivity changes across the human life span: From fetal development to old age. *Journal of Neuroscience Research, 99*(1), 236–262. https://doi.org/10.1002/JNR.24669

Fischl, B. (2012). FreeSurfer. *NeuroImage, 62*(2), 774–781. https://doi.org/10.1016/J.NEUROIMAGE.2012.01.021

Fletcher, J. L., Makowiecki, K., Cullen, C. L., & Young, K. M. (2021). Oligodendrogenesis and myelination regulate cortical development, plasticity and circuit function. *Seminars in Cell & Developmental Biology, 118*, 14–23. https://doi.org/10.1016/J.SEMCDB.2021.03.017

Genc, S., Tax, C. M. W., Raven, E. P., Chamberland, M., Parker, G. D., & Jones, D. K. (2020). Impact of b-value on estimates of apparent fibre density. *Hum Brain Mapp, 41*(10), 2583–2595. https://doi.org/10.1002/hbm.24964

Gheysen, F., Van Waelvelde, H., & Fias, W. (2011). Impaired visuo-motor sequence learning in developmental coordination disorder. *Research in Developmental Disabilities, 32*(2), 749–756. https://doi.org/10.1016/j.ridd.2010.11.005

Gill, K. K., Lang, D., & Zwicker, J. G. (2022). Cerebellar and brainstem differences in children with developmental coordination disorder: A voxel-based morphometry study. *Frontiers in Human Neuroscience, 16*, Article 921505. https://doi.org/10.3389/FNHUM.2022.921505/BIBTEX

Hardwick, R. M., Rottschy, C., Miall, R. C., & Eickhoff, S. B. (2013). A quantitative meta-analysis and review of motor learning in the human brain. *NeuroImage, 67*, 283–297. https://doi.org/10.1016/j.neuroimage.2012.11.020

Hodge, S. M., Makris, N., Kennedy, D. N., Caviness, V. S., Howard, J., McGrath, L., Steele, S., Frazier, J. A., Tager-Flusberg, H., & Harris, G. J. (2010). Cerebellum, language, and cognition in autism and specific language impairment. *Journal of Autism and Developmental Disorders, 40*(3), 300–316. https://doi.org/10.1007/S10803-009-0872-7/TABLES/4

Horowitz, A., Barazany, D., Tavor, I., Bernstein, M., Yovel, G., & Assaf, Y. (2015). In vivo correlation between axon diameter and conduction velocity in the human brain. *Brain Structure and Function, 220*(3), 1777–1788. https://doi.org/10.1007/S00429-014-0871-0/FIGURES/4

Janacsek, K., Fiser, J., & Nemeth, D. (2012). The best time to acquire new skills: Age-related differences in implicit sequence learning across the human lifespan. *Developmental Science, 15*(4), 496–505. https://doi.org/10.1111/j.1467-7687.2012.01150.x

Janacsek, K., & Nemeth, D. (2013). Implicit sequence learning and working memory: Correlated or complicated? *Cortex, 49*(8), 2001–2006. https://doi.org/10.1016/J.CORTEX.2013.02.012

Janacsek, K., Shattuck, K. F., Tagarelli, K. M., Lum, J. A. G., Turkeltaub, P. E., & Ullman, M. T. (2020). Sequence learning in the human brain: A functional neuroanatomical meta-analysis of serial reaction time studies. *NeuroImage, 207*. https://doi.org/10.1016/j.neuroimage.2019.116387

Jeurissen, B., Tournier, J. D., Dhollander, T., Connelly, A., & Sijbers, J. (2014). Multi-tissue constrained spherical deconvolution for improved analysis of multi-shell diffusion MRI data. *NeuroImage, 103*. https://doi.org/10.1016/j.neuroimage.2014.07.061

Kellner, E., Dhital, B., Kiselev, V. G., & Reisert, M. (2016). Gibbs-ringing artifact removal based on local subvoxel-shifts. *Magnetic Resonance in Medicine, 76*(5), 1574–1581. https://doi.org/10.1002/MRM.26054

Knopman, D., & Nissen, M. J. (1991). Procedural learning is impaired in Huntington's disease: Evidence from the serial reaction time task. *Neuropsychologia, 29*(3), 245–254. https://doi.org/10.1016/0028-3932(91)90085-M

Koch, F. S., Sundqvist, A., Thornberg, U. B., Nyberg, S., Lum, J. A. G., Ullman, M. T., Barr, R., Rudner, M., & Heimann, M. (2020). Procedural memory in infancy: Evidence from implicit sequence learning in an eye-tracking paradigm. *Journal of Experimental Child Psychology, 191*, Article 104733. https://doi.org/10.1016/J.JECP.2019.104733

Lebel, C., Treit, S., & Beaulieu, C. (2019). A review of diffusion MRI of typical white matter development from early childhood to young adulthood. *NMR in Biomedicine, 32*(4), Article e3778. https://doi.org/10.1002/NBM.3778

Lieberman, M. D. (2000). Intuition: A social cognitive neuroscience approach. *Psychological Bulletin, 126*(1), 109–136. https://doi.org/10.1037/0033-2909.126.1.109

Lüdecke, D., & Lüdecke, M. D. (2015). *Package "sjPlot."*.

Lum, J. A. G. (2020). Incidental learning of a visuo-motor sequence modulates saccadic amplitude: Evidence from the serial reaction time task. *Journal of Experimental Psychology: Learning Memory and Cognition, 46*(10), 1881–1891. https://doi.org/10.1037/XLM0000917

Lum, J. A. G., Conti-Ramsden, G., Morgan, A. T., & Ullman, M. T. (2014). Procedural learning deficits in specific language impairment (SLI): A meta-analysis of serial reaction time task performance. *Cortex, 51*(1), 1–10. https://doi.org/10.1016/J.CORTEX.2013.10.011

Lum, J. A. G., Gelgic, C., & Conti-Ramsden, G. (2010). Procedural and declarative memory in children with and without specific language impairment. *International Journal of Language & Communication Disorders, 45*(1), 96–107. https://doi.org/10.3109/13682820902752285

Lum, J. A. G., Lammertink, I., Clark, G. M., Fuelscher, I., Hyde, C., Enticott, P. G., & Ullman, M. T. (2019). Visuospatial sequence learning on the serial reaction time task modulates the P1 event-related potential. *Psychophysiology, 56*(2). https://doi.org/10.1111/psyp.13292

Maestrini, L., Hui, F. K., & Welsh, A. H. (2024). Restricted maximum likelihood estimation in generalized linear mixed models. *arXiv preprint arXiv:2402.12719*.

Morgan, O. P., Slapik, M. B., Iannuzzelli, K. G., LaConte, S. M., Lisinski, J. M., Nopoulos, P. C., … Marvel, C. L. (2021). The cerebellum and implicit sequencing: Evidence from cerebellar ataxia. *The Cerebellum, 20*(2), 222–245. https://doi.org/10.1007/s12311-020-01206-7

Nissen, M. J., & Bullemer, P. (1987). Attentional requirements of learning: Evidence from performance measures. *Cognitive Psychology, 19*(1), 1–32. https://doi.org/10.1016/0010-0285(87)90002-8

Palesi, F., De Rinaldis, A., Castellazzi, G., Calamante, F., Muhlert, N., Chard, D., Tournier, J. D., Magenes, G., D'Angelo, E., & Wheeler-Kingshott, C. A. M. G. (2017). Contralateral cortico-ponto-cerebellar pathways reconstruction in humans in vivo: implications for reciprocal cerebro-cerebellar structural connectivity in motor and non-motor areas. *Scientific Reports 2017 7:1*, *7*(1), 1–13. Doi: 10.1038/s41598-017-13079-8.

Penhune, V. B., & Steele, C. J. (2012). Parallel contributions of cerebellar, striatal and M1 mechanisms to motor sequence learning. In *Behavioural Brain Research* (Vol. 226, Issue 2, pp. 579–591). Doi: 10.1016/j.bbr.2011.09.044.

R Core Team. (2022). *R: A language and environment for statistical computing*. Vienna, Austria: R Foundation for Statistical Computing. https://www.R-project.org/.

Raffelt, D. A., Smith, R. E., Ridgway, G. R., Tournier, J. D., Vaughan, D. N., Rose, S., Henderson, R., & Connelly, A. (2015). Connectivity-based fixel enhancement: Whole-brain statistical analysis of diffusion MRI measures in the presence of crossing fibres. *NeuroImage, 117*, 40–55. https://doi.org/10.1016/j.neuroimage.2015.05.039

Raffelt, D. A., Tournier, J. D., Smith, R. E., Vaughan, D. N., Jackson, G., Ridgway, G. R., & Connelly, A. (2017). Investigating white matter fibre density and morphology using fixel-based analysis. *NeuroImage, 144*, 58–73. https://doi.org/10.1016/J.NEUROIMAGE.2016.09.029

Robertson, E. M. (2007). The serial reaction time task: implicit motor skill learning? *Journal of Neuroscience, 27*(38), 10073–10075. https://doi.org/10.1523/JNEUROSCI.2747-07.2007

Shaw, P., Weingart, D., Bonner, T., Watson, B., Park, M. T. M., Sharp, W., Lerch, J. P., & Chakravarty, M. M. (2016). Defining the neuroanatomic basis of motor coordination in children and its relationship with symptoms of attention-deficit/hyperactivity disorder. *Psychological Medicine, 46*(11), 2363–2373. https://doi.org/10.1017/S0033291716000660

Siegert, R. J., Taylor, K. D., Weatherall, M., & Abernethy, D. A. (2006). Is implicit sequence learning impaired in Parkinson's disease? A meta-analysis. *Neuropsychology, 20*(4). https://doi.org/10.1037/0894

Smith, R. E., Connelly, A., & Dhollander, T. (2019). On the regression of intracranial volume in Fixel-based analysis. *Proceedings of the International Society for Magnetic Resonance in Medicine Scientific Meeting and Exhibition*. https://www.researchgate.net/publication/332857716.

Thomas, K. M., Hunt, R. H., Vizueta, N., Sommer, T., Durston, S., Yang, Y., & Worden, M. S. (2004). *Evidence of Developmental Differences in Implicit Sequence Learning: An fMRI Study of Children and Adults*.

Tournier, J. D., Smith, R., Raffelt, D., Tabbara, R., Dhollander, T., Pietsch, M., Christiaens, D., Jeurissen, B., Yeh, C. H., & Connelly, A. (2019). MRtrix3: A fast, flexible and open software framework for medical image processing and visualisation. *NeuroImage, 202*, Article 116137. https://doi.org/10.1016/J.NEUROIMAGE.2019.116137

Ullman, M. T., & Pierpont, E. I. (2005). Specific language impairment is not specific to language: The procedural deficit hypothesis. *Cortex, 41*(3), 399–433. https://doi.org/10.1016/S0010-9452(08)70276-4

Van Dyck, D., Deconinck, N., Aeby, A., Baijot, S., Coquelet, N., De Tiège, X., & Urbain, C. (2022). Atypical procedural learning skills in children with developmental coordination disorder. *Child Neuropsychology*. https://doi.org/10.1080/09297049.2022.2152433/SUPPL_FILE/NCNY_A_2152433_SM1857.DOCX

Veraart, J., Novikov, D. S., Christiaens, D., Ades-Aron, B., Sijbers, J., & Fieremans, E. (2016). Denoising of diffusion MRI using random matrix theory. *Neuroimage, 142*, 394–406. https://doi.org/10.1016/j.neuroimage.2016.08.016

Wasserthal, J., Neher, P. F., Hirjak, D., & Maier-Hein, K. H. (2019). Combined tract segmentation and orientation mapping for bundle-specific tractography. *Medical Image Analysis, 58*, Article 101559. https://doi.org/10.1016/J.MEDIA.2019.101559

Wasserthal, J., Neher, P., & Maier-Hein, K. H. (2018). TractSeg - Fast and accurate white matter tract segmentation. *NeuroImage, 183*, 239–253. https://doi.org/10.1016/J.NEUROIMAGE.2018.07.070

Wickham, H. (2011). ggplot2. *Wiley Interdisciplinary Reviews: Computational Statistics, 3*(2), 180–185. https://doi.org/10.1002/WICS.147

Wickham, H., Averick, M., Bryan, J., Chang, W. D. L., Mcgowan, A., François, R., Grolemund, G., Hayes, A., Henry, L., Hester, J., Kuhn, M., Lin Pedersen, T., Miller, E., Bache, S. M., Müller, K., Ooms, J., Robinson, D., Seidel, D. P., & Yutani, H. (2019). Welcome to the Tidyverse. *Journal of Open Source Software, 4*(43), 1686. https://doi.org/10.21105/JOSS.01686